

Ordered-Defect Sulfides as Thermoelectric Materials

ANDREAS KALTZOGLU,¹ PAZ VAQUEIRO,¹ TRISTAN BARBIER,²
EMMANUEL GUILMEAU,² and ANTHONY V. POWELL^{1,3}

1.—Department of Chemistry, University of Reading, Whiteknights, Reading RG6 6AD, UK.
2.—Laboratoire CRISMAT, UMR 6508 CNRS/ENSICAEN, 6 bd du Maréchal Juin, 14050 Caen
Cedex 4, France. 3.—e-mail: a.v.powell@reading.ac.uk

The thermoelectric behavior of the transition-metal disulfides *n*-type NiCr₂S₄ and *p*-type CuCrS₂ has been investigated. Materials prepared by high-temperature reaction were consolidated using cold-pressing and sintering, hot-pressing in graphite dies or spark-plasma sintering in tungsten carbide dies. The consolidation conditions have a marked influence on the electrical transport properties. In addition to the effect on sample density, altering the consolidation conditions results in changes to the sample composition, including the formation of impurity phases. Maximum room-temperature power factors were 0.18 mW m⁻¹ K⁻² and 0.09 mW m⁻¹ K⁻² for NiCr₂S₄ and CuCrS₂, respectively. Thermal conductivities of ca. 1.4 W m⁻¹ K⁻¹ and 1.2 W m⁻¹ K⁻¹ lead to figures of merit of 0.024 and 0.023 for NiCr₂S₄ and CuCrS₂, respectively.

Key words: Thermoelectric properties, transition-metal sulfides, hot-pressing, spark plasma sintering, consolidation methods

INTRODUCTION

Thermoelectric materials are of increasing interest for applications involving energy harvesting from waste heat. The efficiency of a thermoelectric device is dependent on the physical properties of the component materials. In particular, the thermoelectric performance of a material is dependent on an unusual combination of high electrical conductivity (σ), typically found in metals, together with low thermal conductivity (κ) and high Seebeck coefficient (S), characteristics more usually associated with nonmetallic systems, and is embodied in the dimensionless figure of merit, $ZT = S^2\sigma T/\kappa$.¹ Recently, there has been renewed interest in sulfide-based thermoelectrics and the potential they offer as low-cost alternatives to the current commercial material of choice, Bi₂Te₃.

In the search for sulfide-based thermoelectrics, we have recently begun to investigate the potential of ordered-defect phases. These materials comprise two-dimensional dichalcogenide slabs of edge-sharing

octahedra stacked in a direction perpendicular to the slab direction. The van der Waals' gap between adjacent slabs consists of a network of vacant octahedral and tetrahedral sites. Partial occupancy of such sites by cations in phases, A_xMS₂, may occur in an ordered fashion, giving rise to a range of two-dimensional superstructures,² some of which are stable over a range of x . The nature of the cation ordering is also temperature dependent, and order-disorder transitions are commonly observed at elevated temperatures.^{3–5} Ordered-defect phases are attractive candidate thermoelectrics as they combine low-dimensionality, intrinsic to the dichalcogenide slab, with the capacity to tune electron transport properties through chemical substitution; For example, substitution of vanadium for chromium in NiCr₂S₄ (Ni_{0.5}CrS₂) effects a semiconductor-to-metal transition at a critical level of substitution, $x_c \approx 0.4$.^{6,7}

Here, we present a preliminary investigation of the thermoelectric properties of NiCr₂S₄ and CuCrS₂, each of which contains CrS₂ slabs. The former adopts a monoclinic structure at room temperature⁸ in which 50% of the octahedral sites between pairs of dichalcogenide slabs are occupied by cations

(Received July 1, 2013; accepted October 24, 2013;
published online December 24, 2013)

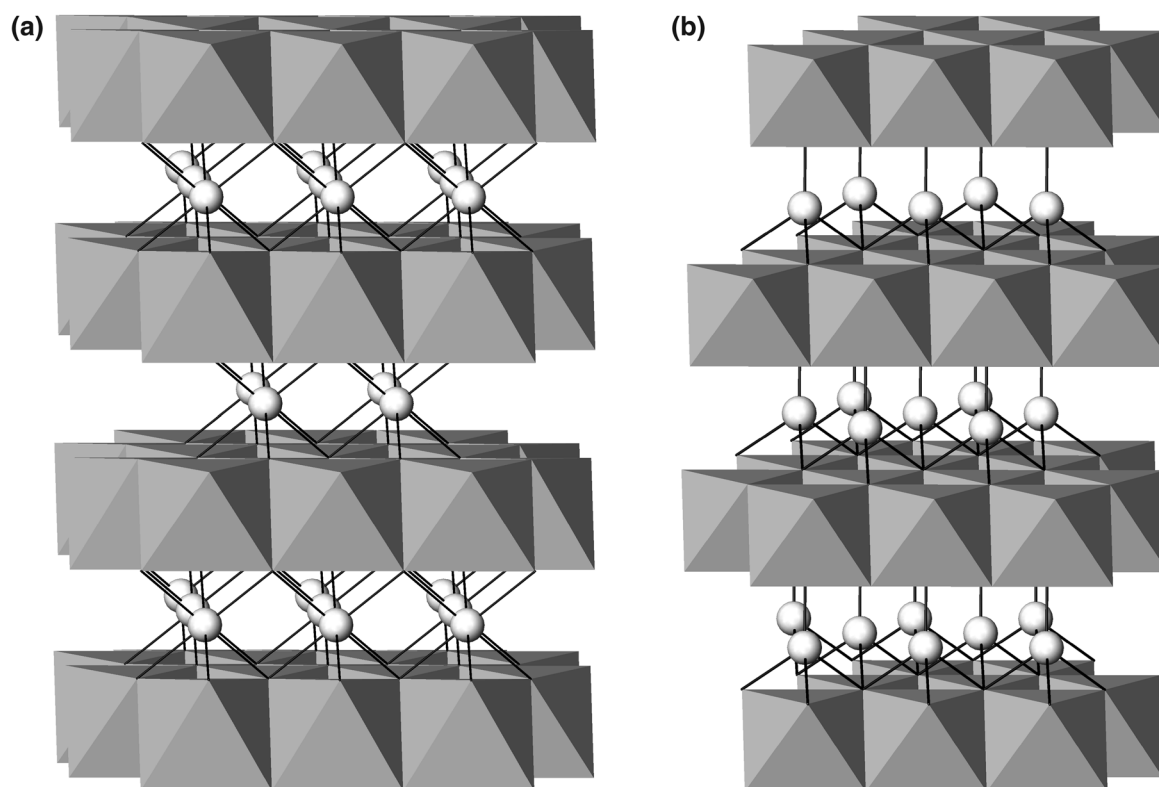


Fig. 1. Crystal structure of (a) NiCr_2S_4 and (b) CuCrS_2 with Ni and Cu atoms (open circles) partially filling octahedral and tetrahedral holes, respectively, between edge-sharing CrS_6 octahedra (grey).

(Fig. 1a). At room temperature, CuCrS_2 adopts a trigonal structure⁹ in which 50% of tetrahedral sites are occupied between pairs of CrS_2 slabs (Fig. 1b). Our previous measurements of the electrical transport properties of cold-pressed and sintered samples of NiCr_2S_4 revealed *n*-type semiconducting behavior and led to the determination of a thermoelectric power factor of ca. $0.1 \text{ mW m}^{-1} \text{ K}^{-2}$ at room temperature.¹⁰ However, to the best of our knowledge, the thermal conductivity of this phase has not been determined. The thermoelectric properties of *p*-type CuCrS_2 have been the subject of considerable recent interest following the report of a figure of merit as high as 2.0 at room temperature.^{11,12} The performance of this material appears to be sensitive to the thermal history of the sample. Extended sintering at high temperature (850°C to 900°C) followed by quenching in air appears to be required for optimum properties, as it promotes copper-ion disorder, thereby reducing the thermal conductivity, and leads to increased texture of the sample, which increases the electrical conductivity. However, recent work by another group has shown that spark plasma sintering (SPS)-processed samples exhibit a much higher electrical resistivity than previously reported with a maximum figure of merit of $ZT = 0.11$ being observed at 400°C .¹³ At higher temperatures, volatilization of sulfur was observed, leading to a reduced charge carrier concentration and a transition from *p*- to *n*-type conductivity.

Herein, we describe an investigation of the impact of the consolidation method on the thermoelectric properties of NiCr_2S_4 and CuCrS_2 . The results demonstrate that the consolidation method has a marked effect on the materials' properties through grain growth, which manifests itself in differences in the degree of densification and through changes in the chemical composition of the sample, including the formation of impurity phases, which can produce variations in the electrical transport properties by up to an order of magnitude and even induce a change in the dominant charge carriers from electrons to holes.

EXPERIMENTAL PROCEDURES

Materials were synthesized by reaction of appropriate mixtures of the elements Ni (99.9%; Aldrich), Cu (99.5%; Aldrich), Cr (99+%; Aldrich), and S (99.99+%; Aldrich) at high temperatures in evacuated ($<10^{-4}$ Torr) silica tubes. In the case of the nickel-containing phase, a reaction mixture slightly deficient in sulfur was used, corresponding to the composition $\text{NiCr}_2\text{S}_{3.93}$, whereas for the copper-containing materials the reaction mixture was stoichiometric. NiCr_2S_4 was heated at 900°C for 1 day before annealing at 500°C for 5 h, whilst CuCrS_2 was heated at 500°C for 12 h. CuCrS_2 was also synthesized by mechanical alloying (MA) in a Retsch PM100 planetary ball mill, using a steel jar

and grinding balls at 650 rpm for 24 h. Powder x-ray diffraction data for all materials were collected using a Bruker D8 Advance powder diffractometer, operating with Ge-monochromated Cu $K_{\alpha 1}$ radiation ($\lambda = 1.5406 \text{ \AA}$) and equipped with a LynxEye linear detector. Rietveld refinements were performed using the GSAS software package.¹⁴

With the exception of one batch of NiCr_2S_4 that was micronized by ball milling (1 h at 400 rpm) and the sample of CuCrS_2 made by MA, all materials were ground to fine powder in an agate mortar prior to consolidation. Powdered samples were consolidated by cold-pressing at 750 MPa in a stainless-steel die followed by sintering for 4 days at 800°C in an evacuated sealed silica tube, by hot-pressing (HP) in a graphite die for 30 min under N_2 atmosphere at various temperatures and pressures, and by SPS on an FCT instrument using tungsten carbide dies under 300 MPa and at various temperatures. Details of temperatures and pressures are provided in the “Results and Discussion” section. Sulfur analysis for selected samples was carried out by inductively coupled plasma–atomic emission spectroscopy (Exeter Analytical, UK).

Rectangular ingots with approximate dimensions of 2 mm \times 2 mm \times 10 mm were cut from the compacted pellets and polished with fine sandpaper. The electrical resistivity (four-probe DC) and Seebeck coefficient of the ingots were determined in the temperature range of 40°C $\leq T \leq$ 300°C under static He atmosphere of 1.1 bar to 1.4 bar using a Linseis LSR-3 instrument. Corresponding data for NiCr_2S_4 consolidated by SPS were obtained over the temperature range of 30°C $\leq T \leq$ 300°C using an Ulvac ZEM-3 instrument. The thermal conductivity of NiCr_2S_4 at room temperature was measured using a TPS 2500s instrument, whereas that of CuCrS_2 was determined using a Quantum Design Physical Property Measurement System.

RESULTS AND DISCUSSION

Materials Characterization

Rietveld analysis of powder x-ray diffraction data confirmed that all reaction products were phase-pure materials. Powder diffraction data for NiCr_2S_4 could be well described (Fig. 2) by a monoclinic structural model involving complete ordering of Ni and Cr over octahedral sites. It was not possible to refine the sulfur content, owing to the small deviation from stoichiometry. Rietveld refinement using powder x-ray diffraction data collected for CuCrS_2 (Fig. 3) revealed that Cu and Cr atoms were fully ordered at tetrahedral and octahedral sites, respectively.

The density of the consolidated samples of NiCr_2S_4 increased with increasing consolidation temperature and pressure (Table I), reaching ca. 99% of the crystallographic density when processed by SPS (650°C, 300 MPa). Notably, powder x-ray diffraction data for consolidated samples revealed ca. 5 wt.% of NiS_2 impurity in the samples consolidated by HP at

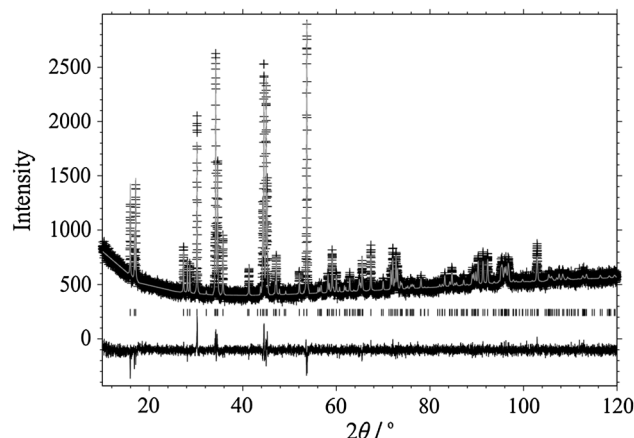


Fig. 2. Final observed (crosses), calculated (solid line), and difference (full lower line) profiles from Rietveld refinements for NiCr_2S_4 using powder x-ray diffraction data [space group: $I2/m$, $a = 5.91128(8) \text{ \AA}$, $b = 3.41042(5) \text{ \AA}$, $c = 11.1094(1) \text{ \AA}$, $\beta = 91.163(1)^\circ$; $R_{\text{wp}} = 4.90\%$, $\chi^2 = 1.26$].

100 MPa and by SPS at 300 MPa. The presence of NiS_2 is consistent with the increased sulfur content determined by elemental analysis of the sample processed by HP at 100 MPa. The absence of any chromium-containing decomposition products in the powder x-ray diffraction data suggests that this phase can tolerate a degree of nonstoichiometry on the nickel and sulfur sublattices. The sample processed by HP at 600°C and 60 MPa exhibited a sulfur content slightly lower than that expected from the reaction stoichiometry, suggesting that some volatilization may occur under these conditions.

The density of the consolidated samples of CuCrS_2 ranged from 89% to 97% of the crystallographic value (Table II). Under the same HP conditions, the density of the MA sample was slightly higher than for the sample obtained by conventional reaction. Powder x-ray diffraction indicated that no sample decomposition occurred under any of the consolidation conditions investigated. However, powder x-ray diffraction data for the sample produced by cold-pressing exhibited a marked increase in the intensity of (00 l) reflections (Fig. 3b), suggesting preferred orientation due to texturing. This is consistent with previous reports¹¹ which suggest that texturing occurs on prolonged high-temperature sintering followed by fast quenching of the polycrystalline solid.

Physical Properties

The electrical resistivity and Seebeck coefficient data for NiCr_2S_4 (Fig. 4) reveals a marked dependence of the electrical transport properties on the consolidation method. Whilst electrons are the dominant charge carriers in all consolidated materials, the resistivity of HP samples changes from a semiconducting to a metallic-like temperature

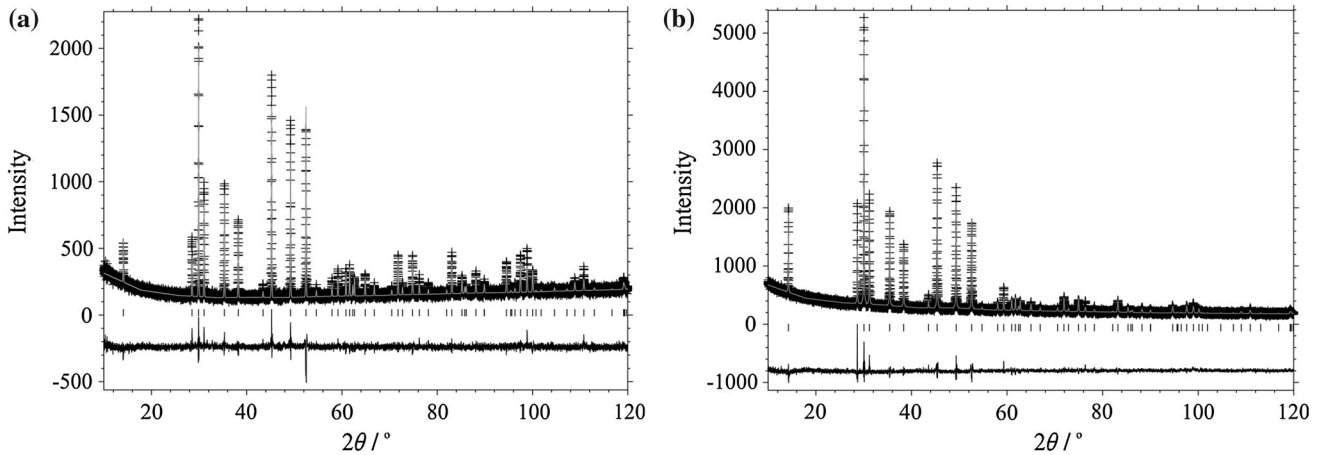


Fig. 3. Final observed (crosses), calculated (solid line), and difference (full lower line) profiles from Rietveld refinements for (a) as-synthesized CuCrS_2 using powder x-ray diffraction data [space group: $R\bar{3}$, $a = 3.47962(2)$ Å, $c = 18.6927(2)$ Å, $R_{\text{wp}} = 8.63\%$, $\chi^2 = 1.37$] and (b) cold-pressed and sintered CuCrS_2 , illustrating the change in reflection intensities due to texturing [space group: $R\bar{3}$, $a = 3.48038(3)$ Å, $c = 18.6969(2)$ Å, $R_{\text{wp}} = 7.36\%$, $\chi^2 = 1.63$].

Table I. Consolidation conditions and bulk characteristics for NiCr_2S_4 samples

Consolidation Conditions	Code	Density (g cm^{-3}) ^b	S Content (wt.%) ^c	Impurity Phases
HP at 600°C/60 MPa	1a	3.31	43.52	None detected
HP at 600°C/110 MPa	2a	3.61	45.15	NiS_2
HP at 600°C/60 MPa ^a	3a	3.16	–	None detected
HP at 680°C/60 MPa	4a	3.68	–	None detected
HP at 800°C/60 MPa	5a	3.72	–	None detected
SPS at 600°C/300 MPa	6a	4.18	–	NiS_2 detected
SPS at 650°C/300 MPa	7a	4.27	–	NiS_2 detected

^aPowder ball milling at 400 rpm for 1 h prior to hot pressing; ^bCrystallographic density: $d = 4.31 \text{ g cm}^{-3}$; ^c43.65 wt.% S content expected for $\text{NiCr}_2\text{S}_{3.93}$ and 44.08 wt.% for NiCr_2S_4 .

Table II. Consolidation conditions and density for CuCrS_2 samples

Consolidation Conditions	Code	Density (g cm^{-3}) ^b
Cold pressing at 700 MPa, sintered 4 days at 850°C, quenched	1b	4.06
Hot pressing at 600°C, 60 MPa	2b	4.15
Hot pressing at 600°C, 60 MPa ^a	3b	4.23
Hot pressing at 650°C, 100 MPa	4b	4.44

^aObtained by MA; ^bCrystallographic density: $d = 4.56 \text{ g cm}^{-3}$.

dependence with increasing density, whereas the two SPS-processed samples exhibit semiconducting behavior. The Seebeck coefficient at 40°C ranged from $-18 \mu\text{V K}^{-1}$ to $-172 \mu\text{V K}^{-1}$ depending on the processing method. For the SPS-processed samples, the absolute value of the Seebeck coefficient decreases with increasing temperature, whereas for most of the hot-pressed samples the Seebeck coefficient increased in absolute value with increasing temperature. The temperature dependence of the electrical resistivity and Seebeck coefficient of the hot-pressed samples is characteristic of conduction

by extrinsic charge carriers and indicates that these samples behave as degenerate semiconductors. The highest power factor of $0.18 \text{ mW m}^{-1} \text{ K}^{-2}$ at room temperature was reached for the material processed by SPS at 650°C and 300 MPa, being higher than that determined in our previous report on cold-pressed and sintered pellets.¹⁰ This difference may be attributed to the lower relative density (ca. 75%) of the latter material, which leads to an increase in the electrical resistance (by a factor of 2) over the SPS-processed sample. The thermal conductivity of NiCr_2S_4 processed by HP at 680°C and 60 MPa was

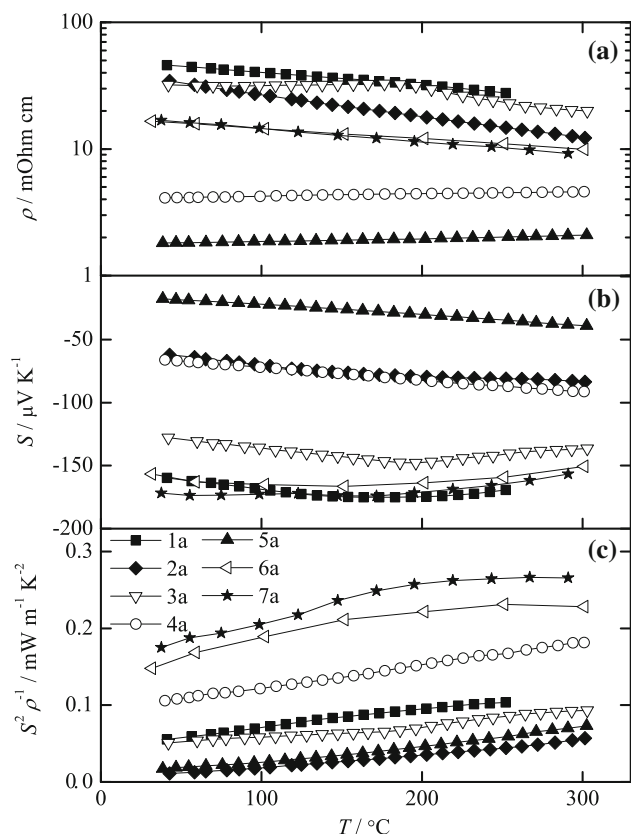


Fig. 4. Thermoelectric properties of NiCr_2S_4 over the temperature range of $30^\circ\text{C} \leq T \leq 300^\circ\text{C}$: (a) electrical resistivity on logarithmic scale, (b) Seebeck coefficient, and (c) power factor.

determined to be $1.4 \text{ W m}^{-1} \text{ K}^{-1}$ at 40°C , leading to a figure of merit of $ZT \approx 0.024$.

All consolidated samples of CuCrS_2 behave as *p*-type semiconductors (Fig. 5). The Seebeck coefficient of HP samples shows an almost linear increase with temperature, whereas for the cold-pressed and sintered sample the value is almost temperature independent. In the latter case, a power factor of $0.09 \text{ mW m}^{-1} \text{ K}^{-2}$ and thermal conductivity measured as $\kappa(40^\circ\text{C}) \approx 1.2 \text{ W m}^{-1} \text{ K}^{-1}$ lead to $ZT \approx 0.023$ at room temperature. This performance is much lower than that in the original report by Tewari et al.¹¹ ($\rho = 6 \text{ mOhm cm}$, $S = 445 \mu\text{V K}^{-1}$, $\kappa = 0.48 \text{ W m}^{-1} \text{ K}^{-1}$, and $ZT = 2$ at room temperature) but is in good agreement with a large number of literature reports on the thermoelectric properties of this phase.^{13,15–17} The principal origin of this discrepancy is believed to be the strong anisotropy in the cold-pressed and sintered sample.⁹ The bond strength between Cu cations in the van der Waals' gap and S anions in the CrS_2 slabs has a significant effect on the Cu^+ ionic conductivity.¹⁸ The increase in unit cell volume upon prolonged sintering, observed here* and in a previous

*The lattice parameters increase from $a = 3.47962(2) \text{ \AA}$, $c = 18.6927(2) \text{ \AA}$ for an as-synthesized sample to $a = 3.48038(3) \text{ \AA}$, $c = 18.6969(2) \text{ \AA}$ for a cold-pressed and sintered sample.

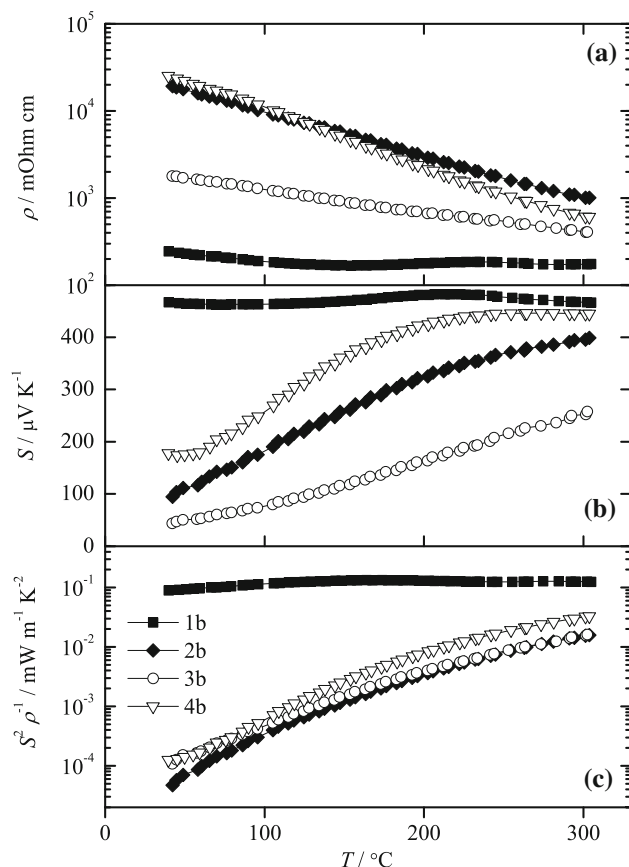


Fig. 5. Thermoelectric properties of CuCrS_2 over the temperature range of $40^\circ\text{C} \leq T \leq 300^\circ\text{C}$: (a) electrical resistivity on logarithmic scale, (b) Seebeck coefficient, and (c) power factor.

study where the *c* parameter increased upon sintering at 900°C for 8 days,⁹ may be indicative of a weakening of this bonding and increased mobility of Cu^+ species. The formation on consolidation of point defects associated with the copper-ion sublattice may also influence the electrical properties,¹⁹ although if present, these are at too low a level to be detected in Rietveld refinement using powder x-ray diffraction data.

CONCLUSIONS

Both NiCr_2S_4 and CuCrS_2 exhibit a modest thermoelectric response. The highest measured power factor of $0.27 \text{ mW m}^{-1} \text{ K}^{-2}$ at 267°C for the SPS-processed sample of NiCr_2S_4 is considerably lower than for the best *n*-type materials such as the skutterudite $\text{Yb}_{0.19}\text{Co}_4\text{Sb}_{12}$,^{20,21} which exhibits a power factor of up to $4 \text{ mW m}^{-1} \text{ K}^{-2}$ at 300°C . However, there is considerable scope for tuning the thermoelectric properties of ordered-defect phases through chemical substitution, to which such materials are particularly amenable. The work reported here also demonstrates that the consolidation process may have a marked effect on the thermoelectric properties of NiCr_2S_4 and CuCrS_2 . Variations in electron transport properties of up to an order of magnitude

are observed depending on the consolidation conditions used. In addition to changes in sample composition that are evidenced by powder x-ray diffraction, variations in sample density occur. These are likely to reflect changes in the microstructure of the materials involving differences in grain growth and grain boundary formation. Detailed examination by microscopy techniques is required to characterize such changes at the microstructural level.

ACKNOWLEDGEMENTS

Financial support by the European Commission (FP7-SME-2012-1, Grant Agreement No. 315019) is gratefully acknowledged. We wish to thank Drs. Lars Hålldahl, K-Analys AB, Sweden and Ramzy Daou, Laboratoire CRISMAT, France for thermal conductivity measurements.

REFERENCES

- J.R. Sootsman, D.Y. Chung, and M.G. Kanatzidis, *Angew. Chem. Int. Ed.* 48, 8616 (2009).
- P. Vaqueiro and A.V. Powell, *Chem. Mater.* 12, 2705 (2000).
- P. Vaqueiro, S. Hull, B. Lebech, and A.V. Powell, *J. Mater. Chem.* 9, 2859 (1999).
- P. Vaqueiro, A.V. Powell, and B. Lebech, *Phys. B* 276, 238 (2000).
- I.G. Vassilieva, T.Yu. Kardash, and V.V. Malakhov, *J. Struct. Chem.* 50, 288 (2009).
- R.J. Bouchard and A. Wold, *J. Phys. Chem. Solids* 27, 591 (1966).
- A.V. Powell, P. Vaqueiro, and A. McDowall, *Solid State Ion.* 172, 469 (2004).
- A.V. Powell, D.C. Colgan, and C. Ritter, *J. Solid State Chem.* 134, 110 (1997).
- G.C. Tewari, T.S. Tripathi, and A.K. Rastogi, *Z. Kristallogr.* 225, 471 (2010).
- A.V. Powell, P. Vaqueiro, and T. Ohtani, *Phys. Rev. B* 71, 125120 (2005).
- G.C. Tewari, T.S. Tripathi, and A.K. Rastogi, *J. Electron. Mater.* 39, 1133 (2010).
- G.C. Tewari, T.S. Tripathi, P. Kumar, A.K. Rastogi, S.K. Pasha, and G. Gupta, *J. Electron. Mater.* 40, 2368 (2011).
- Y.-X. Chen, B.-P. Zhang, Z.-H. Ge, and P.-P. Shang, *J. Solid State Chem.* 186, 109 (2012).
- A.C. Larson, and R.B. von Dreele, General Structure Analysis System, Los Alamos Laboratory, [Report LAUR 85-748] (1994).
- C.-G. Han, B.-P. Zhang, Ge Z-H, L.-J. Zhang, and Y.-C. Liu, *J. Mater. Sci.* 48, 4081 (2013).
- G.M. Abramova, A.M. Vorotynov, G.A. Petrakovskii, N.I. Kiselev, D.A. Velikanov, A.F. Bovina, R.F. Al'mukhametov, R.A. Yakshibaev, and É.V. Gabitov, *Phys. Solid State* 46, 2225 (2004).
- N. Le Nagard, G. Collin, and O. Gorochoy, *Mater. Res. Bull.* 14, 1411 (1979).
- R.F. Almukhametov, R.A. Yakshibaev, E.V. Gabitov, A.R. Abdullin, and R.M. Kutusheva, *Phys. Stat. Sol. B* 236, 29 (2003).
- M.A. Boutbila, J. Rasneur, and M.E. Aatmani, *J. Alloys Compd.* 283, 88 (1999).
- G.S. Nolas, M. Kaeser, R.T. Littleton, and T.M. Tritt, *Appl. Phys. Lett.* 77, 1855 (2000).
- J. Garcia-Canadas, A.V. Powell, A. Kaltzoglou, P. Vaqueiro, and G. Min, *J. Electron. Mater.* 42, 1369 (2013).